Variability of natural low flow magnitudes in the Upper Colorado River Basin: Identifying monotonic and periodic trends, and relative role of large-scale climate dynamics

Maryam Pournasiri Poshtiri and Indrani Pal*

**College of Engineering and Applied Science, Department of Civil Engineering, University of Colorado Denver, 1200 Larimer Street, Campus Box 116, Denver CO 80204. E-mail – indrani.pal@ucdenver.edu. Phone: +1 303 352 3894*

Abstract

Low flow magnitude in a head water basin is important for planners because minimum available amount of water in a given time period often leads to serious repercussions, in both up and the downstream regions. This concern is common in the arid territory like Colorado River basin located in the southwestern United States. Low flow variability in Colorado River is due to complex interactions between several natural and anthropogenic factors but here we aim to identify trends and systematic variability of low flows, and the relative role of large-scale climate dynamics at different spatial locations of the basin. The research questions we aim to answer are: *How variable are the low flow conditions in the headwater basin of Colorado River? Did location-specific low flow change in the past years? How are low flows linked with synoptic ocean-atmospheric conditions?* Towards that aim we select 17 stream gauge locations, which are identified as "undisturbed" stream gauges meaning that these stations represent near-natural river flow regimes in the headwater area of Colorado River providing a useful resource for assessment of large-scale climate dynamics and local hydrology associations without the confounding factor of major direct (e.g. water abstraction) or indirect (e.g. land-use change) human modification of flows. A detailed diagnostic analysis gave us fair understanding on the variability and changes in low flow magnitude that is explained by large-scale ocean-atmospheric conditions. Most notably, eastern and western parts of Upper Colorado River Basin (UCRB) indicated opposite trending patterns of low flows—the west (east) showing drier (wetter) conditions, and the low flow magnitudes were specifically found to be having multi-decadal variability revealing the close associations with Interdecadal Pacific Oscillation or Pacific Decadal Oscillation (PDO) patterns.

Key words: low flow, variability, Colorado River, large-scale climate dynamics

1. Introduction

Variability and change in stream flow can directly influence water supply (both quantity and quality) for domestic, agricultural, industrial, ecological, and other needs. Palmer et al. (2008) indicated that river discharge in every inhabited river basin in the world would face changes; some will have large increases while others will likely face the water scarcity. Understanding variability of the volume of stream flow is important because very high flows can cause damaging floods and erosion, while very low flows can fail to provide adequate water supply, diminish water quality, and affect important ecological services (Smakhtin, 2001). Existing evidence suggest that water scarcity due to low river flow could be one of the main drivers of societal and cross-boundary conflicts (Gleick and Palaniappan, 2010; Gleick, 2010, 2014). Thus, anticipating the magnitudes of seasonal and annual minimum flow in the headwater locations of a river is important for up and downstream water management purposes. Intricate connections between human and natural processes influence the water supply from the basin headwater and as such minimum river flow is a result of complex interactions between human and biophysical features and thus, differing from one region to another (Jones et al., 2012). Hence, characterizing lower tail of river flow distribution demands more attention than it has received so far.

Water resources in the southwestern United States, are especially scarce and climatic changes may cause significant alterations in water availability, quality, and demand. The hydrology of the southwest is already characterized by strong variability on seasonal to multiannual time scales, reflecting its sensitivity to fluctuations in large-scale atmospheric circulation patterns from the Pacific Ocean, the Gulf of California, and the Gulf of Mexico (Seager et al., 2007). Amongst major river basins, Colorado River is the critical source of water for 7 states in the arid southwestern United States (especially for high aggregated demand met in the municipal, agricultural, and industrial sectors), and that, this river has a history of going under low flow conditions (i.e. flow going under a minimum threshold condition) in the past (USGS, 2004; Meko et al., 2007; Ellis et al., 2010; Gleick, 2010). In addition, population growth, agricultural, urban, and industrial expansions within the past decades enhanced this effect. It has been reported in the scientific literature that the Colorado River flow is expected to reduce further under future warming scenarios due to a combination of strong temperature-induced runoff curtailment, reduced annual precipitation, and increased (potential) evapo-transpiration (Milly et al., 2005; Christensen and Lettenmeier, 2007; Seager et al., 2007), and consequently the seasonal distribution of flow will also change due to changing ratio of snow to total precipitation as well as changing timing of the snow melt (Fritze et al., 2011). Another risk to Colorado River stream flow is multi-decadal droughts, which is also expected to change under climate change (IPCC AR5, 2013). Therefore, impacts of drought conditions on the river flows, especially in the driest time, are also expected to change. But, little is known regarding how the low flow characteristics changed over time in response to changes in the climate.

There is complexity and heterogeneity of low flow dynamics in a river basin. Therefore, it is difficult to generalize characterization of low flow. Low flow, defined in many different ways (section II in SI), could be a sole or combination of multiple factors in different seasons. Such factors may include slowly flowing ground water discharge, surface discharge from lakes, marshes, snow-pack dynamics, melting glaciers, basin precipitation, basin temperature and evaporation rates, basin soil, topography, geology and vegetation, river channel characteristics, and various man-induced effects (Smakhtin, 2001). For instance, in the summer time (July through October), low flows of most part of the United States, are usually derived by base flow (Reilly and Kroll, 2003; Flynn, 2003). On the other hand, in cold or mountainous regions, low flows are subject to the spatial influences of ice, snow or glacier melting in addition to the usual basin parameters, which is also true for Colorado River flow (Smakhtin, 2001; Reilly and Kroll, 2003; Miller and Piechota, 2011; Curran et al., 2012; EPA, 2012). Here we hypothesize that, like meteorological droughts, large-scale climate dynamics is also linked with low flow variability but some characteristics of low flow might vary across locations due to variable physiographic parameters.

This hypothesis leads to the science questions: *How variable are the low flow conditions in the headwater basin of Colorado River? Did location-specific low flow change in the past years? How are low flows linked with synoptic ocean-atmospheric conditions?*

Through the Colorado River Compact, the Upper Colorado River Basin (UCRB) supplies water and hydropower for much of the southwestern United States and hence low flow dynamics of UCRB has large influence on both the up and the downstream water supply. These scientific questions will enable us to understand the statistical characteristics of regional low flow variability in this important river basin as well as capture their physical connections to large-scale ocean-atmospheric systems. Our research findings will support scientists and engineers to develop prediction tools that assist in climate informed and timely water management decisions during potential crises, as well as maintaining the minimum flow conditions in the river to sustain ecosystem services.

The paper proceeds as follows. Section 2 describes the datasets used, section 3 summarizes calculation of low flow statistics, section 3 explains results, relevant methods used, and related discussions, and section 4 summarizes the findings.

2. Data

We selected 17 "undisturbed" stream gauges in UCRB, which primarily contribute to the largest amount of total Colorado River stream flow (McCabe et al., 2007; Gao et al., 2011). Consideration of the undisturbed stations minimizes the human induced effects on the natural flow and captures natural variability and changes. We downloaded the daily river flow data from USGS Hydro-Climatic Data Network 2009 (Lins, 2012). The detailed description of the data, including the homogeneity/quality, is found in the supplementary information (SI) (section I). Table 1-A lists the stations' information and Figure 1 shows the geographic locations of those stations as well as the length of the data ranging from 25 to 61 years. As evident in Figure 1, the Upper Colorado River Basin (UCRB) differs in topographical features, notably the eastern stream gauges are located in the higher elevation areas than the western locations, also indicated in Table 1.

To study large-scale climatological patterns, we used global Surface Temperature (ST) and Mean Sea Level Pressure (MSLP) data from 1949-2011 from NCEP/NCAR reanalysis V1.0 monthly diagnostic products (Kalnay et al., 1996). We downloaded these datasets in ready to analyze format from the International Research Institute for Climate and Society Data Library (http://iridl.ldeo.columbia.edu).

3. Calculation of low flow statistics

To calculate the low flow statistics, we considered climate years that extends from April 1–March 31, as suggested by previous research (Ries and Friesz, 2000; Flynn, 2003; Reilly and Kroll, 2003; Pyrce, 2004; Risley et al., 2008; Martin and Arihood, 2010; Curran et al., 2012; EPA, 2012). Daily mean flows for all complete climatic years of record are used to determine low-flow statistics for all 17 stream-gaging stations. Low-flows in streams can be characterized in many ways but in the United States, the 7-day low flow—annual or seasonal series of the smallest values of mean discharge over any 7-consecutive days (q7)—is a common method for determining the low flow magnitude (Ries and Friesz, 2000; Smakhtin, 2001; Flynn, 2003; Pyrce, 2004; Reilly and Kroll, 2003; Risley et al., 2008; Martin and Arihood, 2010; Curran et al., 2012; EPA, 2012). We followed this approach in this research. Annual q7 generally occurs in the driest season, mainly in the beginning of spring and/or summer for UCRB. But, different stream gauges experience q7 in different months (Table S1). Because the summer time low flow conditions is generally driven by the base flow in most part of the United States, and in winter, that subjects to the influences of ice, snow or glacier melting, it is also crucial to study the variations of low flows in different seasons in addition to annual low flows. In this research we also considered four traditional seasons, namely Dec-Jan-Feb (DJF), Mar-Apr-May (MAM), Jun-Jul-Aug (JJA), and Sep-Oct-Nov (SON).

4. Results and Discussions

This section presents an in depth descriptive analysis of low flow statistics at UCRB locations (4.1). That helps to detect the seasonal and annual variability patterns and trends of q7, thus answering the first two research questions. Following that we report the results of a correlational investigation that identify relationships between low flow statistics and large-scale climatic patterns, answering the third research question (4.2).

4.1. Low flow variability and trends

Figure 2 shows variation of annual q7 magnitude—annual smallest values of mean discharge over any 7-consecutive days, and those for the traditional seasons are shown in Figure S1. Figure

2 (and Figure S1) indicates that annual (and seasonal) low flow magnitudes within UCRB have high spatio-temporal variability. This is expected because the river basin characteristics, especially the topographical features and the source of water (whether snow-melt or precipitation induced runoff) play a major role for q7 variation. Particularly, the variability differs in the east and west sides of the basin (separated by -107.5^0 long) where the elevations also differ, as also indicated in Figure S2. In addition, spatial variability of q7 is quantified in Table 1-B for annual and Tables S2-S5 for the traditional seasons.

Of the major assumptions in a correlational study is normal distribution idea. Since q7 falls at an extreme tail of the daily mean flow distribution, non-normal behavior can be expected. Therefore, to detect the non-normal behavior in q7 time series for different stream gauge locations, we estimated skewness and kurtosis values and reported them in the summary statistics tables. As those values indicate, annual and seasonal q7 distributions are normal in general, because, as a rule of thumb, they have an absolute skewness value less than 3 and an absolute kurtosis value less than 10.

To determine co-variability, we conducted a cross correlation analysis between q7 time series for different stream gauge stations. Tables 2 and 3 list the annual and JJA cross-correlation analysis results and Tables S6-S8 list the other results. These tables indicate that q7 magnitudes in most stations are positively correlated with each other; which is most prominent and statistically significant for the cases in the summer (JJA), as in Table 3, and followed by SON (Table S8). This finding indicates that variability of low flow at multiple locations might be linked with common external factors, for JJA in particular. Generally, stations close to each other yield highest positive significant correlations.

Monotonic and periodic trends assessment: Impacts of global change and large-scale natural climate variability is felt locally. Therefore, it is imperative to look at whether there have been any significant monotonic trends and sub/multi decadal patterns in seasonal and annual low flow statistics and how they compare amongst locations. Periodicity is the indicator for small-scale hydrological system response to large-scale circulation patterns, such as El-Nino Southern Oscillation (ENSO) or Pacific Decadal Oscillation (PDO). We considered non-parametric Mann-Kendall trend tests to detect monotonic trends and wavelet analysis to identify periodicity or multi-decadal patterns.

The Mann–Kendall test is applicable to the detection of a monotonic trend in a time series with no seasonal or other cycle. Mann (1945) formulated the non-parametric test for monotonic trend detection, and Kendall (1975) derived the test statistic distribution for testing non-linear trend and turning point. This method allows us to ignore high-frequency (i.e. multiple change point) variations. Since there are chances of outliers in the low flow data, non-parametric Mann–Kendall test is useful because its statistic is based on the sign of differences, not directly on the values of the random variable, and therefore, the trends determined are less affected by the outliers. On the other hand, Wavelet analysis has been widely used to analyze time series data with localized variations of power. This method decomposes a one dimensional time series (or frequency spectrum) into two dimensional time-frequency spaces in order to analyze signals of the data containing non-stationary power at many different frequencies and creates the time-scaled output signal (Torrence and Compo, 1998). We used an interactive web toolkit developed by C. Torrence and G. Compo that uses Mortlet wavelet basis function, incorporates the edge effects due to finite-length time series in a cone of influence, and includes a statistical significance testing using specific theoretical wavelet spectra for both white noise and red-noise processes (http://ion.researchsystems.com).

Figure 3 depicts the monotonic trend results for different time intervals (indicated in Table 1-A) and Figure S3 indicates the same but for those stations which have more than 30-years of data permitting more statistical power, both of which reveal identical behavior where the trends in low-flow magnitudes exhibit variable nature in different seasons and annually. Stations, which are located close to each other, are generally showing homogeneity in significant trends. More specifically, we notice a clear distinction in monotonic trends in the eastern and the western sides of -107.5^{o} longitude. Annual, DJF, MAM, and SON q7 trends are negative on the west side and positive on the east side. JJA q7 trends are usually negative everywhere, except some non-significant positive trends. Negative trending patterns in the western part of UCRB, are consistent with some of the previous studies, which indicated a general trend of low flow states toward permanently drier conditions in the southwestern US due to a projected decrease in runoff and soil moisture in the headwaters of Colorado river arising from a projected increase in (potential) evap-transpiration (USGS, 2004; McCabe et al., 2007; Gleick, 2010; Seager et al., 2007, 2013). However, positive trend patterns on the eastern part of UCRB, which has higher elevation, does not follow the idea that "dry will get drier and wet will get wetter". This monotonic trend study indicates the importance of locally based studies needing further investigations to detect the causes for the differences in trends other than diverse physiographic characters of the basin (Figure 1).

Hydro-climatic analysis have also indicated that there is considerable non-stationarity in measured and reconstructed stream flow estimates for the Colorado River basin, which may be linked with inter-decadal, decadal, multi-decadal and even secular variations in ocean temperatures (Cook et al., 2004; Gray et al., 2004; Hidalgo, 2004; McCabe et al., 2004). To detect periodic trends in low flow magnitude, wavelet analysis was performed. The decomposition of time series into time-frequency space permits the identification of the dominant modes of variability and determining how these modes vary in time. A few examples of periodicity of q7 magnitudes are shown in Figure 4, all of which indicate close to 10-16 years periods. Rest of the test results for other stations is presented in the Tables S9-S10, which also confirms recurrent 10-16 years periodicity of q7 data. Though the exact cause of these multi-decadal variations is not fully understood yet, which will require longer datasets, we hypothesize that this dominant periodicity might be closely related to Interdecadal Pacific Oscillation (IPO) or Pacific Decadal Oscillation (PDO) patterns of northern Pacific (Zhang et al., 1997; Folland et al., 2002; Dai, 2013), as further established in the following section.

4.2. Linkage with Large-Scale Climate Patterns

This section summarizes Pearson correlation patterns between common variability of low flow magnitudes (q7) across the study basin and large-scale climate variables. We've considered global surface temperature (ST) anomalies and mean sea level pressure (MSLP) anomalies to determine variability of q7 dictated by climate. To do that, first, we conducted the Principal Component Analysis (PCA) to determine the transformed time series that are orthogonal to each other and explaining the common variance of q7 across the stations within UCRB, both for traditional seasons and annually. This analysis requires the data having equal length, thus, we considered only those stations having more than 30-years length. Thus, 14 stations having data from 1976-2011 were considered for PCA.

Figure S4 indicates the variance explained by the Principal Components (PCs) of annual and seasonal q7. PC1 explains around 40-60% of the variance in the UCRB data for different time frames considered, and then the explained variance drops gradually by the other PCs. Figure 5 (Figure S5) shows the correlation between annual (seasonal) PC1 and the global average climate in northern summer (Apr-May-Jun-Jul-Aug-Sept/AMJJAS) and northern winter (Oct-Nov-Dec-Jan-Feb-Mar/ONDJFM). We considered two distinct northern hemisphere seasons to check which timing of the year indicates recognized ocean-atmospheric signals. Figure 5 indicates that PC1 of annual q7 has distinct associations with the summer season climate, most notably, a positively correlated ENSO-like surface temperature pattern extending from the coast of China to the Central Northern Pacific surrounded by a negatively correlated horseshoe type pattern in the summer and a negatively correlated ENSO-like surface temperature region in the tropical Pacific is visible (also indicated by the positively correlated MSLP in the same region and season). DJF, MAM, and SON seasons also yielded similar results as annual with little different patterns for JJA PC1. These prominent sea surface temperature patterns in the northern Pacific (especially pole ward of 20° N) indicate Pacific Decadal Oscillation (PDO) type behavior. The influence of distinct phases of PDO on dominant mode of UCRB low flows is consistent with McCabe et al. (2004) who indicated the effect of this multi-decadal ocean-atmospheric patterns on the drought frequency across the US, especially over the Southwestern United States. A direct correlation analysis yielded statistically significant associations between the northern hemispheric summer season PDO indices and the annual (-0.40), DJF (-0.41), MAM (-0.48), JJA (-0.31) and SON (-0.40) time series of PC1 respectively. PDO shifts phases on at least inter-decadal time scale, usually about 20 to 30 years. The Interdecadal Pacific Oscillation (IPO), on the other hand, displays similar sea-surface temperature and sea-level pressure (SLP) patterns with the PDO but with a cycle of about 15–30 years. This, along with the wavelet analysis results above, convincingly indicate that IPO might be associated closely with the prominent variability of the annual low flows; i.e. at the positive (negative) phase of PDO/IPO the magnitude of q7 would be decreased (increased), also indicating a related greater (lesser) frequency or magnitude of droughts supporting McCabe et al. (2004) and Dai (2013)'s drought related finding but from the perspective of low flows.

Many studies previously indicated persistent La Nina-like cold SST anomalies in the tropical central and eastern Pacific Ocean leading to below-normal precipitation and often droughts over Southwestern North America (e.g., Seager et al., 2005; Mo et al., 2009; Wang et al., 2010). Because El-Nino Southern Oscillation (ENSO) associates with the PDO, an ENSO type pattern is evidently allied with the low flow variability in Figure 5 and S5. Therefore, this study re-establishes the connections between the variability of annual and seasonal droughts, but now via study from the context of low flow magnitudes, and the northern hemispheric summer time ocean-atmospheric patterns such as ENSO/PDO/IPO.

5. Summary

Low-flow statistics for the streams is important for water supply planning and design, waste-load allocation, reservoir storage design, and maintenance of quantity and quality of water for irrigation, recreation, and wildlife conservation. Colorado River is the lifeline for many states in the arid southwestern US. Water availability in the headwater basin matters a great deal for these states. In this study we aim to understand the variability and changes in low flow conditions during different seasons and annually as well as to detect what role the large-scale ocean-atmospheric features play to modulate them. Since low flow is due to a complex mixture of many local physiographic factors and climatic mechanisms, it has been hard historically to generalize the low flow for the entire basin. However, this study indicates that significant monotonic and periodic trends are existent for annual and seasonal low flow magnitudes but differing in the eastern and the western parts of the basin due to variant topographical conditions (east having higher elevation). Furthermore, the first Principal Component of annual and seasonal low flow magnitudes (q7) across the Upper Colorado River Basin (UCRB) indicates more than 40-60% variability and shows clear connections with the Pacific ocean patterns (PDO/IPO) in northern hemispheric summer season, yielding 10-16 years periodicity. This indicates a greater possibility of statistical predictions of low flow magnitudes using climate indices, which forms our next step of research. A skillful and timely prediction of location specific low flow statistics is important and necessary for environmental, industrial and agricultural sectors, which has an aim to keep up with the water demand for human and ecological systems during the time of water scarcity. This scientific research takes a step forward to contribute to that reason.

Author contribution: I.P. designed the experiments and M.P.P carried out the analysis. I.P. and M.P.P prepared the manuscript.

Acknowledgments. We extend our thanks to Dr. Erin Towler from NCAR and anonymous reviewers for reading the manuscript and providing valuable comments and suggestions, and to Mr. Alejandro Henao for helping to create Figure 1 on GIS platform.

References

Christensen N.S., and Lettenmeier, D.P.: A multimodel ensemble approach to assessment of climate change impacts on the hydrology and water resources of the Colorado River Basin, Hydrology and Earth System Sciences, 11, 1417–1434, 2007.

Cook, E.R., Woodhouse, C.A., Eakin, C.M., Meko, D.M., and Stahle, D.W.: Long-term aridity changes in the western United States, Science, 306, 1015–1018, 2004.

Curran, C.A., Eng, K., and Konrad, C.P.: Analysis of low flows and selected methods for estimating low-flow characteristics at partial-record and ungaged stream sites in western Washington, U.S. Geological Survey, Water-Resources Scientific Investigations Report 2012-5078, 2012.

Dai, A.: The influence of the Inter-decadal Pacific Oscillation on U.S. precipitation during 1923-2010, Climate Dynamics, 41, 633-646, doi: 10.1007/s00382-012-1446-5, 2013.

Ellis, A.W., Goodrich, G.B., and Garfin, G.: A hydroclimatic index for examining patterns of drought in the Colorado River Basin, International Journal of Climatology, 30, 236–255, doi: 10.1002/joc.1882, 2010.

EPA: Background information on the definition and characteristics of low flows, the relationship between low flows and aquatic life criteria, and design flows. Flow 101. DFLOW, http://water.epa.gov/scitech/datait/models/dflow/flow101.cfm, 2012.

Flynn, R.H.: Development of regression equations to estimate flow durations and low-flow-frequency statistics in New Hampshire Streams, U.S. Geological Survey, Water-Resources Investigations Report 02-4298, 2003.

Folland, C.K., Renwick, J.A., Salinger, M.J., and Mullan, A.B.: Relative influences of the Interdecadal Pacific Oscillation and ENSO on the South Pacific Convergence Zone, Geophysical Research Letters, 29, 1643, doi: 10.1029/2001GL014201, 2002.

Fritze, H., Stewart I.T., and Pebesma, E.: Shifts in western North American snowmelt runoff regimes for the recent warm decades, J. Hydrometeor, 12, 989-1006, 2011.

Gao, Y., Vano, J.A., Zhu, C., and Lettenmaier, D.P.: Evaluating climate change over the Colorado River basin using regional climate models, Journal of Geophysical Research, 116, D13104, doi: 10.1029/2010JD015278, 2011.

Gleick, P.H. and Palaniappan, M.: Peak water limits to freshwater withdrawal and use, PNAS 107, 11155–11162, 2010.

Gleick, P.H.: Roadmap for sustainable water resources in southwestern North America, PNAS 107, 21300–21305, 2010.

Gleick, P.H.: Water, Drought, Climate Change, and Conflict in Syria. Weather Climate and Society, doi:10.1175/WCAS-D-13-00059.1, 2014.

Gray, S.T., Graumlich, L.J., Betancourt, J.L., and Pederson, G.T.: A tree-ring based reconstrution of the Atlantic Multidecadal Oscillation since 1567 A.D., Geophysical Research Letters, 31, L12205, doi: 10.1029/2004GL019932, 2004.

Hidalgo, H.G.: Climate precursors of multidecadal drought variability in the Western United States, Water Resources Research 40, W12504, doi: 10.1029/2004WR003350, 2004.

IPCC, AR5: Climate Change 2013: The Physical Science Basis, Contribution of Working Group I to the Fourth Assessment Report of the Intergovernmental Panel on Climate Change, Cambridge University Press, Cambridge, United Kingdom and New York, NY, USA, 2013.

Jones, J.A., Creed, I.F., Hatcher, K.L., Warren, R.J., Adams, M.B., Benson, M.H., Boose, E., Brown, W.A., Campbell, J.L., Covich, A., Clow, D.W., Dahm, C.N., Elder, K., Ford, C.R., Grimm, N.B., Henshaw, D.L., Larson, K.L., Miles, E.S., Miles, K.M., Sebestyen, S.D., Spargo, A.T., Stone, A.B., Vose, J.M., and Williams, M.W.: Ecosystem processes and human influences regulate streamflow response to climate change at long term ecological research sites, American Institute of Biological Sciences, 62, 390-404, 2012.

Kalnay, E. and Coauthors. The NCEP/NCAR 40-Year Reanalysis Project, Bulletin of the American Meteorological Society, 77, 437–471, 1996.

Kendall, M. G.: Rank correlation methods, Charles Griffin, London, 1975.

Lins, H.F.: USGS Hydro-Climatic Data Network 2009 (HCDN–2009), U.S. Geological Survey, Fact Sheet 2012–3047.4 p. , http://pubs.usgs.gov/fs/2012/3047/, 2012.

Mann, H. B.: Non-parametric tests against trend, Econometrica, 13, 245–259, 1945.

Martin, G.R. and Arihood, L.D.: Methods for estimating selected low-flow frequency statistics for unregulated streams in Kentucky, U.S. Geological Survey, Scientific Investigations Report 2010–5217, 83 p, 2010.

McCabe, G.J., Betancourt, J.L., and Hidalgo, H.G.: Associations of decadal to multidecadal sea-surface temperature variability with upper Colorado River flow, Journal of the American Water Resources Association, 43, 183-192, 2007.

McCabe, G.J., Palecki, M.A., and Betancourt, J.L.: Pacific and Atlantic Ocean influences on multidecadal drought frequency in the United States, Proceedings of the National Academy of Sciences, 101, 4136-4141, 2004.

Meko, D.M., Woodhouse, C.A., Baisan, C.A., Knight, T., Lukas, J.J., Hughes, and M.K., Salzer, M.W.: Medieval drought in the upper Colorado River Basin, Geophysical Research Letters, 34, L10705, doi:10.1029/2007GL029988, 2007.

Miller, W.P. and Piechota, T.C.: Trends in Western U.S. snowpack and related upper Colorado River Basin streamflow, American Water Resources Association, 47, 1197–1210, doi:10.1111/j.1752-1688.2011.00565.x, 2011.

Milly, P.C.D., Dunne, K.A., and Vecchia, A.V.: Global pattern of trends in streamflow and water availability in a changing climate: Nature, 438, 347–350, doi:10.1038/nature04312, 2005.

Mo, K.C., Schemm, J.K.E., and Yoo, S.H.: Influence of ENSO and the Atlantic Multidecadal Oscillation on drought over the United States, Journal of Climate, 22, 5962–5982, 2009.

Palmer, M.A., Liermann, C.A.R., Nilsson, C., Florke, M., Alcamo, J., Lake, P.S., and Bond, N.: Climate change and the world's river basins: anticipating management options, Frontiers in Ecology and the Environment, 6, 81–89, doi: 10.1890/060148, 2008.

Pyrce, R.: Hydrological low flow indices and their uses, Watershed Science Centre, Report 04-2004, 2004.

Reilly, C.F. and Kroll, C.N.: Estimation of 7-day, 10-year low-streamflow statistics using baseflow correlation, Water Resources Research 3, 1236, doi: 10.1029/2002WR001740, 2003.

Ries, K.G. and Friesz, P.J.: Methods for estimating low-flow statistics for Massachusetts streams, U.S. Geological Survey, Scientific Investigations Report 00-4135, 2000.

Risley, J., Stonewall, A., and Haluska, T.: Estimating flow-duration and low-flow frequency statistics for unregulated streams in Oregon, U.S. Geological Survey, Scientific Investigations Report 2008–5126, 2008.

Seager, R., Kushnir, Y., Herweijer, C., Naik, N., and Velez, J.: Modeling of tropical forcing of persistent droughts and pluvial over Western North America: 1856–2000, Journal of Climate, 18, 4065–4088, doi: http://dx.doi.org/10.1175/2009JCLI3188.1, 2005.

Seager, R., Ting, M., Held, I., Kushnir, Y., Lu, J., Vecchi, G., Huang, H.P., Harnik, N., Leetmaa, A., Lau, N.C., Li, C., Velez, J., and Naik, N.: Model projections of an imminent transition to a more arid climate in southwestern North America, Science, 316, 1181, doi: 10.1126/science.1139601, 2007.

Seager, R., Ting, M., Li, C., Naik, N., Cook, B., Nakamura, J., and Liu, H.: Projections of declining surface-water availability for the southwestern United States, Nature Climate Change, 3, doi: 10.1038/NCLIMATE1787, 2013.

Smakhtin, V.U.: Low flow hydrology: a review, Journal of Hydrology, 240, 147–186, 2001.

Torrence, C., and Compo, G. P.: A Practical Guide to Wavelet Analysis. Bulletin of the American Meteorological Society. 79 (1), pp. 61–78. 1998.

U.S. Geological Survey (USGS): Climatic fluctuations, drought, and flow in the Colorado River Basin, 2004.

Wang, H., Schubert, S., Suarez, M., and Koster, R. :The physical mechanisms by which the leading patterns of SST variability impact US precipitation, Journal of Climate, 23, 1815–1836, 2010.

Zhang, Y., Wallace, J.M., and Battisti, D.S.: ENSO-like interdecadal variability: 1900–93, Journal of Climate, 10, 1004–1020, 1997.

(A)

(B)

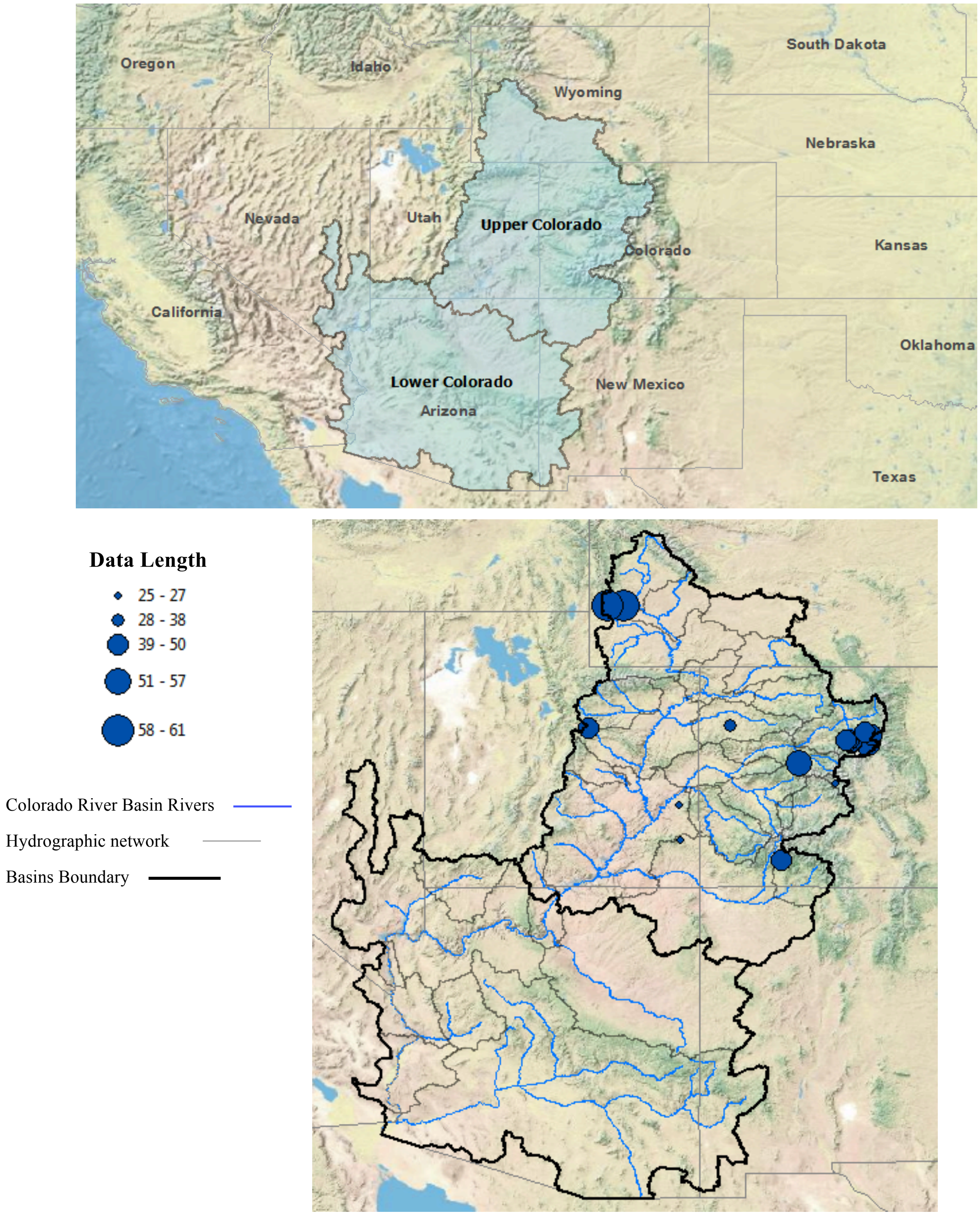

Figure 1: (A) Colorado River basin Location (upper and lower) **(B)** Hydrographic network, major rivers and tributaries, stream gauge stations' locations (blue bubbles), and data length displayed as proportional to the blue bubble diameters.

(A)

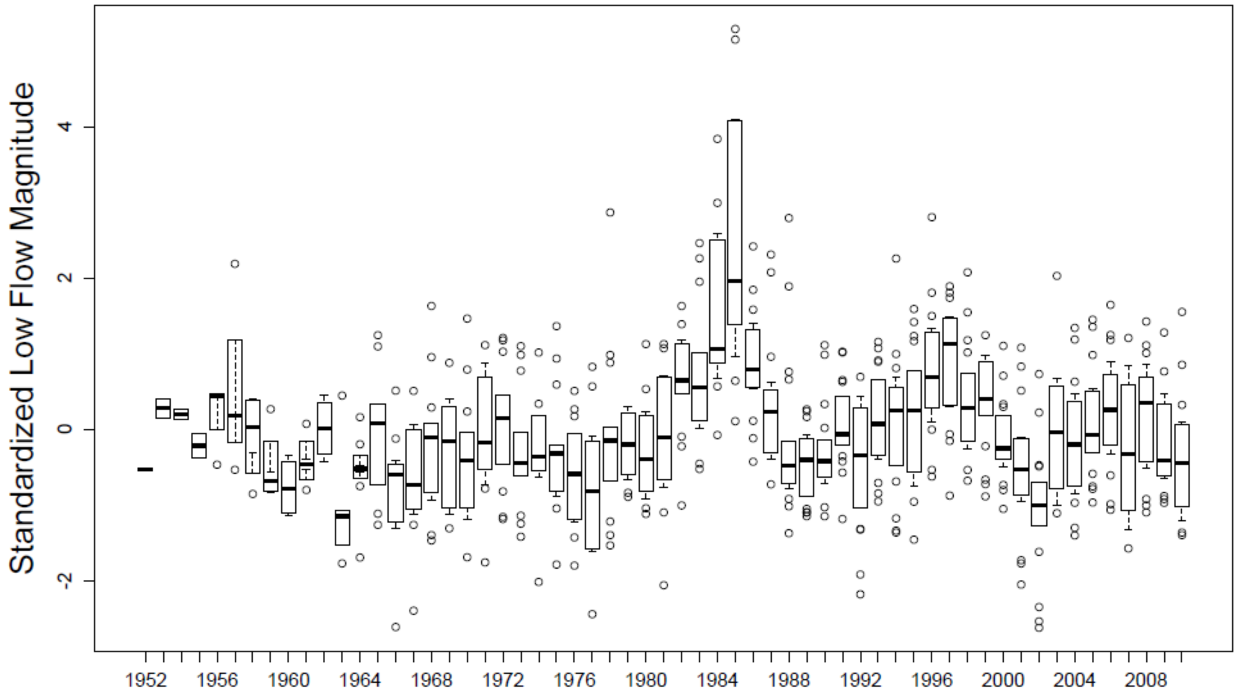

(B)

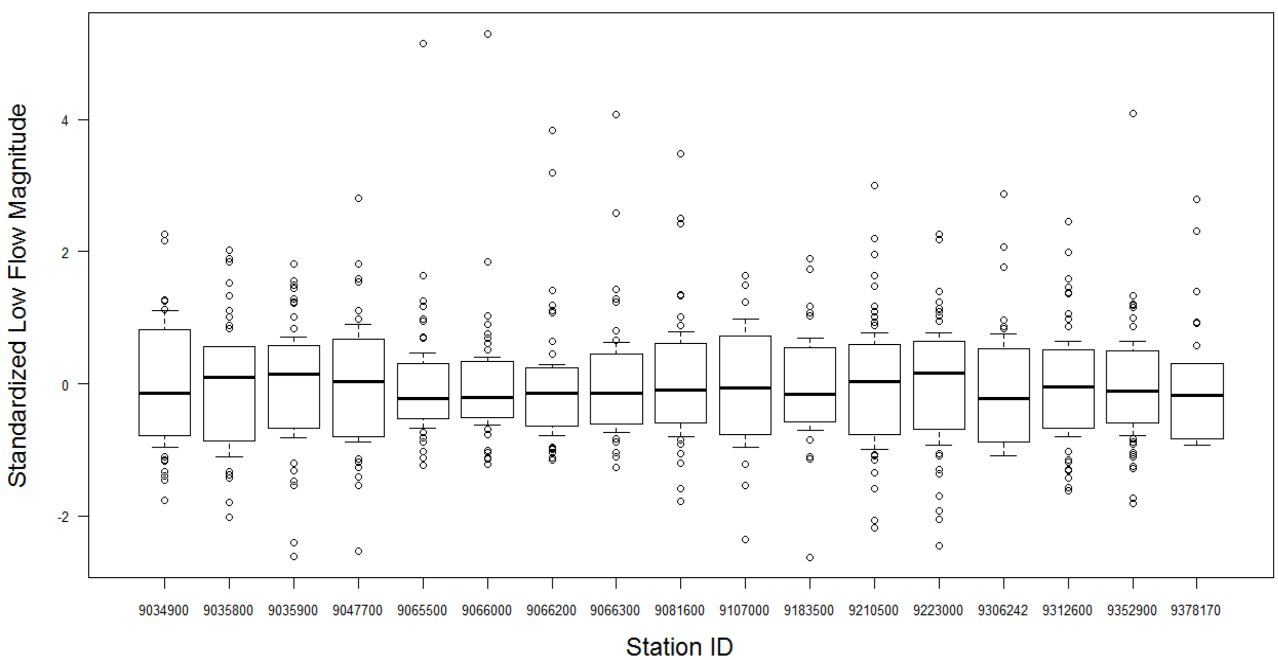

Figure 2: Variability of annual q7 (standardized). **(A)** UCRB while all stations pulled together for every year; **(B)** Individual stations, all years pulled together.

A)

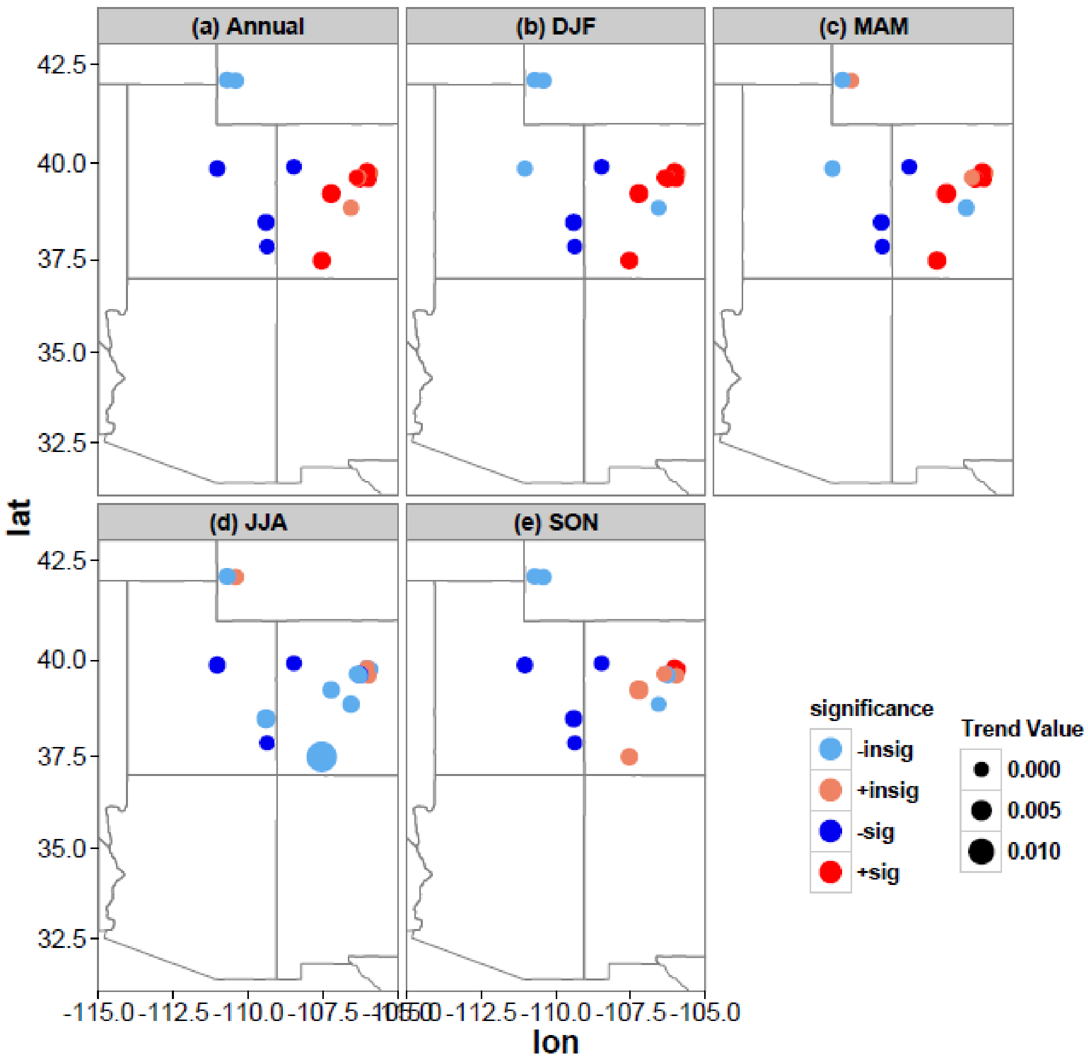

B)

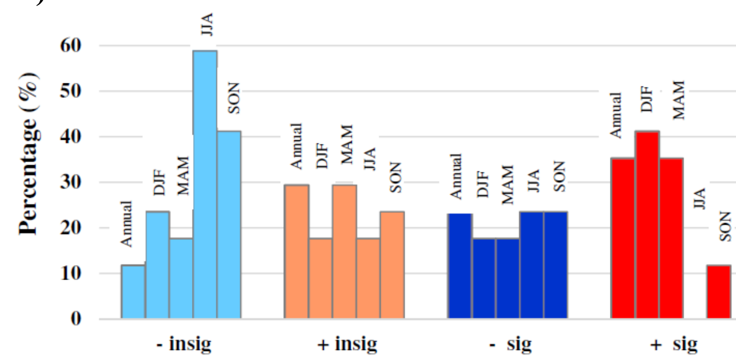

Figure 3: A) Monotonic trends for q7 at each stream-gauge location in cms/day/year. (a) Annual, (b) DJF, (c) MAM, (d) JJA, (e) SON. Color bubbles indicate location of each station, sign and significance of the trend estimates. 90% significant levels are used. The size of the bubble is proportional to the magnitude of the trend. **B)** The bar plots of different types of trends in annual and four different seasons.

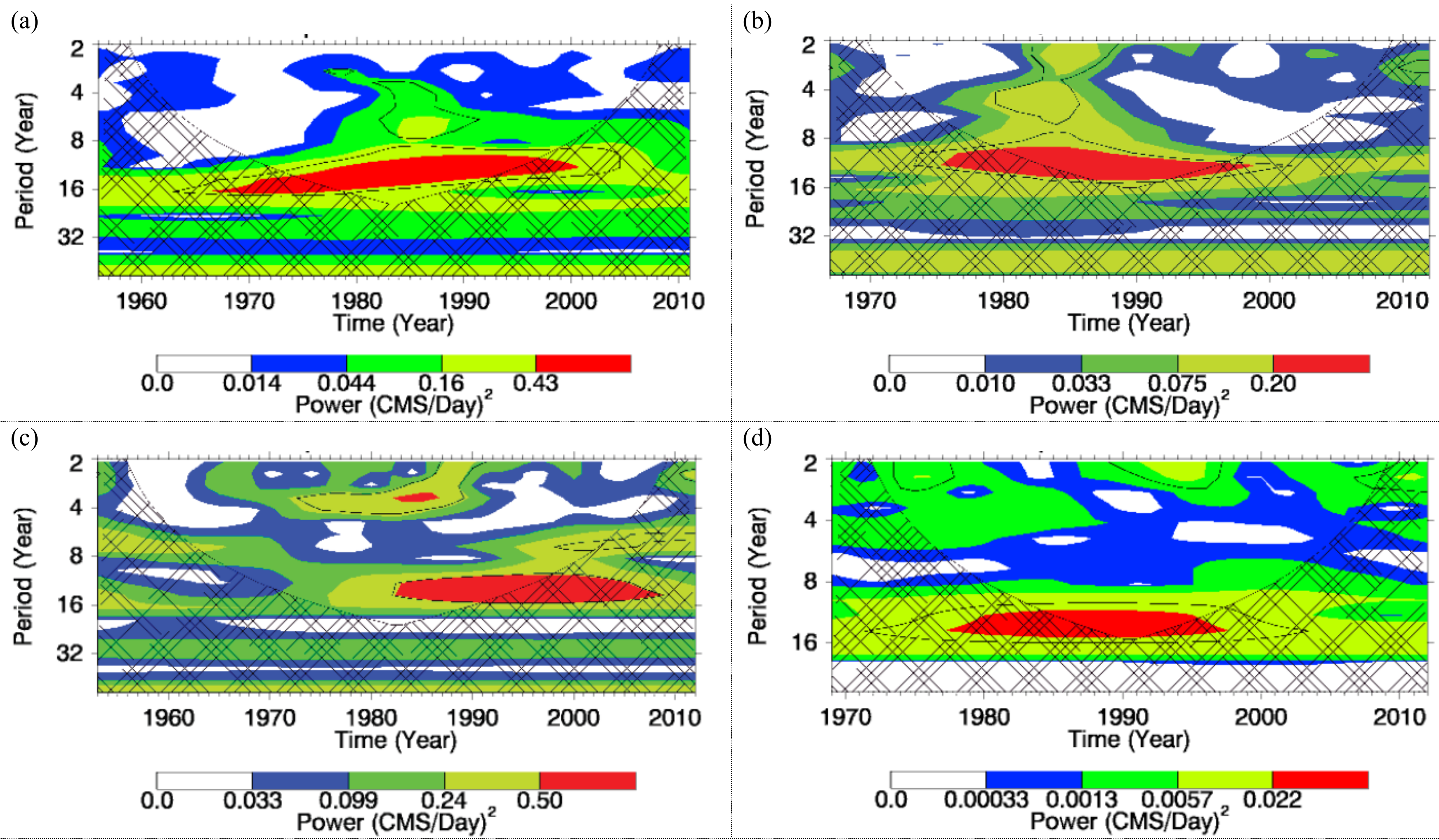

Figure 4: Example periodicity of low flow magnitudes. Wavelet power spectrum for (a) annual q7 time series for Crystal station (east), (b) JJA q7 time series for South Fork station (east), (c) JJA q7 time series for Fontenelle station (west), (d) SON q7 time series for White station (west). The black contours enclose regions of greater than 90% confidence for a red-noise process. Cross-hatched regions indicate the cone of influence (Torrence and Compo, 1998).

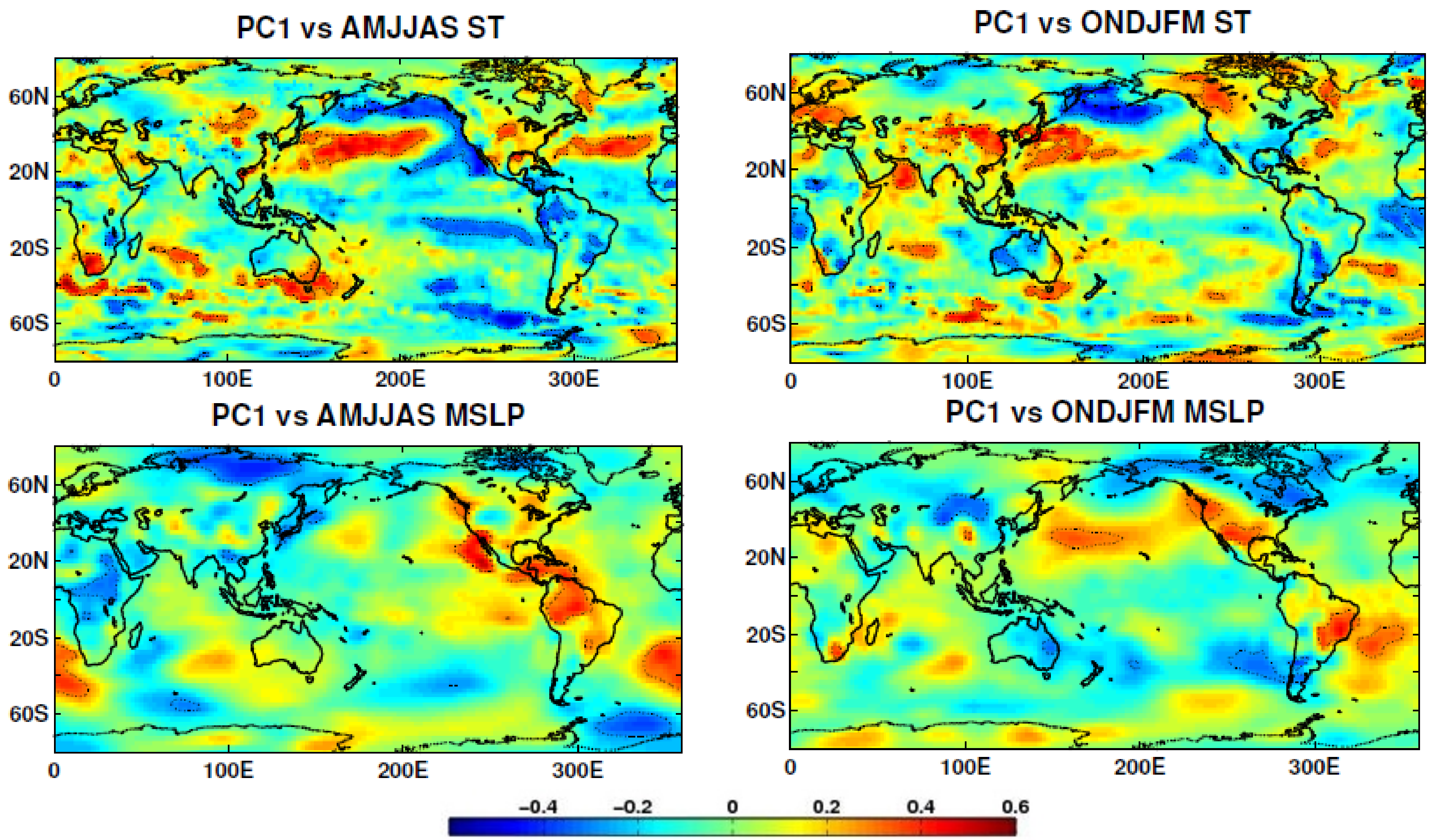

Figure 5: Pearson correlations between PC1 of annual q7 with northern summer (AMJJAS) and northern winter (ONDJFM) climate data (95% significant regions are marked by dotted contours).

Table 1-A: Description of HCDN-2009 streamflow gaging stations in UCRB (Lins, 2012).

Station ID	Station Name	Drainage area in Sq-km	LAT_GAGE	LONG_GAGE	Altitude above NGVD29 (m)	Data available for years	Data length (years)
9066000	Black Gore Creek Near Minturn, CO. (east)	32.409	39.596	-106.265	2788.9	1965-2011	47
9034900	Bobtail Creek Near Jones Pass, CO. (east)	15.649	39.760	-105.906	3179.1	1967-2011	36
9066200	Booth Creek Near Minturn, CO. (east)	16.097	39.648	-106.323	2537.5	1966-2011	46
9306242	Corral Gulch Near Rangely, CO. (west)	81.986	39.920	-108.473	2005.6	1976-2011	36
9081600	Crystal River Ab Avalanche C, Near Redstone, CO. (east)	432.893	39.232	-107.227	2104.6	1957-2011	55
9035800	Darling Creek Near Leal, CO. (east)	22.944	39.801	-106.026	2724.9	1967-2009	43
9065500	Gore Creek At Upper Station, Near Minturn, CO. (east)	37.776	39.626	-106.278	2621.3	1965-2011	47
9047700	Keystone Gulch Near Dillon, CO. (east)	23.570	39.594	-105.973	2849.9	1959-2011	53
9066300	Middle Creek Near Minturn, CO. (east)	15.522	39.646	-106.382	2499.4	1966-2011	46
9035900	South Fork Of Williams Fork Near Leal, CO. (east)	72.842	39.796	-106.031	2728.0	1967-2011	45
9107000	Taylor River At Taylor Park, CO. (east)	331.619	38.860	-106.567	2846.8	1989-2011	23
9352900	Vallecito Creek Near Bayfield, CO. (west)	188.151	37.478	-107.544	2409.8	1964-2011	66
9183500	Mill Creek at Sheley Tunnel, Near Moab, UT. (west)	74.302	38.483	-109.404	1676.4	1989-2011	23
9210500	Fontenelle C Nr Herschler Ranch, Nr Fontenelle, WY. (west)	398.309	42.096	-110.417	2118.4	1953-2011	59
9223000	Hams Fork Below Pole Creek, Near Frontier, WY. (west)	333.153	42.110	-110.710	2272.3	1954-2011	58
9312600	White River Bl Tabbyune C Near Soldier Summit, UT. (west)	195.295	39.876	-111.037	2203.7	1969-2011	43
9378170	South Creek Above Reservoir Near Monticello, UT. (west)	21.898	37.847	-109.370	2185.4	1987-2011	25

Note: CO = Colorado; UT = Utah; WY = Wyoming; LAT_GAGE = Latitude of a streamgauge; LONG_GAGE = Longitude of a streamgauge; NGVD29= National Geodetic Vertical Datum of 1929

Table 1-B: Summary statistics table for annual q7 time series for each stream gauge station in UCRB.

Station ID	Station Name	Mean (cms)	Median (cms)	Standard deviation (cms)	Skewness	Kurtosis
9066000	Black Gore Creek Near Minturn, CO. (east)	0.67	0.65	0.12	0.22	-0.83
9034900	Bobtail Creek Near Jones Pass, CO. (east)	1.73	1.76	0.31	0.08	-0.73
9066200	Booth Creek Near Minturn, CO. (east)	6.73	6.95	1.52	-0.43	-0.11
9306242	Corral Gulch Near Rangely, CO. (west)	1.78	1.79	0.33	0.19	0.04
9081600	Crystal River Ab Avalanche C, Near Redstone, CO. (east)	2.53	2.31	1.01	2.91	9.08
9035800	Darling Creek Near Leal, CO. (east)	2.09	1.89	0.98	2.90	9.19
9065500	Gore Creek At Upper Station, Near Minturn, CO. (east)	0.76	0.71	0.37	1.84	4.30
9047700	Keystone Gulch Near Dillon, CO. (east)	0.23	0.20	0.18	1.70	4.36
9066300	Middle Creek Near Minturn, CO. (east)	42.70	41.93	8.86	1.03	1.76
9035900	South Fork Of Williams Fork Near Leal, CO. (east)	29.15	28.93	3.90	-0.34	-0.58
9107000	Taylor River At Taylor Park, CO. (east)	4.76	4.61	0.94	-0.25	0.25
9352900	Vallecito Creek Near Bayfield, CO. (west)	17.85	18.00	5.35	0.37	0.32
9183500	Mill Creek at Sheley Tunnel, Near Moab, UT. (west)	10.24	10.86	3.94	-0.26	-0.22
9210500	Fontenelle C Nr Herschler Ranch, Nr Fontenelle, WY. (west)	0.43	0.35	0.32	1.05	0.45
9223000	Hams Fork Below Pole Creek, Near Frontier, WY. (west)	2.55	2.47	1.58	0.29	-0.51
9312600	White River Bl Tabbyune C Near Soldier Summit, UT.	17.06	16.43	5.39	1.20	3.73
9378170	South Creek Above Reservoir Near Monticello, UT. (west)	0.05	0.04	0.06	1.24	0.86
Note: CO = Colorado; UT = Utah; WY = Wyoming						

Table 2: Pearson correlation coefficients between annual q7 time series of different stations (1989-2011). 90% statistically significant estimates are shown.

Station ID	9034900	9066200	9306242	9081600	9035800	9065500	9047700	9066300	9035900	9107000	9352900	9183500	9210500	9223000	9312600
9034900															
9066200															
9306242															
9081600															
9035800															
9065500		0.41													
9047700			0.39												
9066300		0.62		0.45			0.38								
9035900		-0.35		0.39											
9107000	0.41						0.50	0.51							
9352900		0.39		0.68				0.37							
9183500			0.56												
9210500			0.40	0.40			0.41		0.44						
9223000			0.38	0.37			0.44						0.66		
9312600				0.41			0.62	0.36	0.37			0.45	0.55	0.64	
9378170			0.64									0.75			
9066000				0.50			0.43				0.41		0.72	0.46	0.43

Table 3: Pearson correlation coefficients between JJA q7 time series of different stations (1989-2011). 90% statistically significant estimates are shown.

Station ID	9034900	9066200	9306242	9081600	9035800	9065500	9047700	9066300	9035900	9107000	9352900	9183500	9210500	9223000	9312600	9378170
9034900	0.73															
9066200	0.81	0.78														
9306242	0.64	0.47	0.47													
9081600	0.74	0.48	0.78	0.58												
9035800	0.61	0.61	0.70	0.58	0.76											
9065500	0.87	0.71	0.86	0.61	0.89	0.78										
9047700	0.78	0.73	0.78	0.41	0.59	0.56	0.76									
9066300	0.83	0.77	0.85	0.48	0.61	0.65	0.74	0.72								
9035900	0.87	0.74	0.80	0.54	0.75	0.62	0.83	0.80	0.83							
9107000	0.82	0.48	0.78	0.61	0.92	0.62	0.90	0.67	0.65	0.77						
9352900	0.68	0.57	0.60	0.55	0.62	0.57	0.69	0.53	0.57	0.47	0.69					
9183500	0.73	0.61	0.77	0.63	0.80	0.77	0.79	0.53	0.60	0.60	0.71	0.67				
9210500	0.63	0.44	0.47	0.58	0.37		0.45	0.58	0.49	0.61	0.49	0.42	0.50			
9223000	0.68	0.49	0.50	0.76	0.54	0.56	0.59	0.60	0.55	0.65	0.56	0.54	0.60	0.87		
9312600	0.70	0.44	0.71	0.72	0.81	0.67	0.72	0.62	0.68	0.74	0.80	0.52	0.72	0.68	0.74	
9378170	0.72	0.70	0.73	0.48	0.69	0.62	0.78	0.60	0.49	0.58	0.62	0.60	0.86	0.43	0.49	0.52

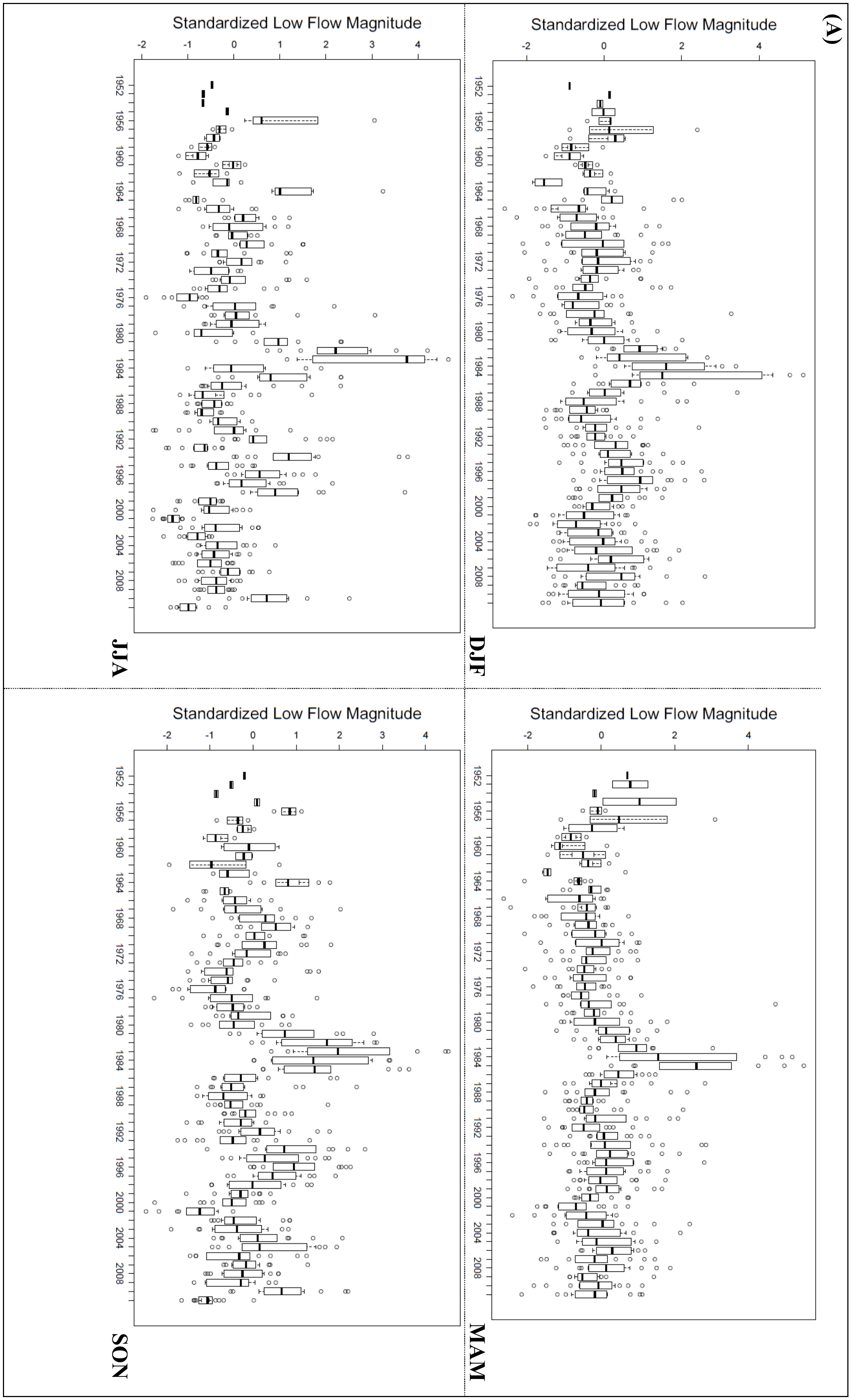

(A)
DJF
JJA
MAM
SON
Standardized Low Flow Magnitude
Standardized Low Flow Magnitude
Standardized Low Flow Magnitude
Standardized Low Flow Magnitude

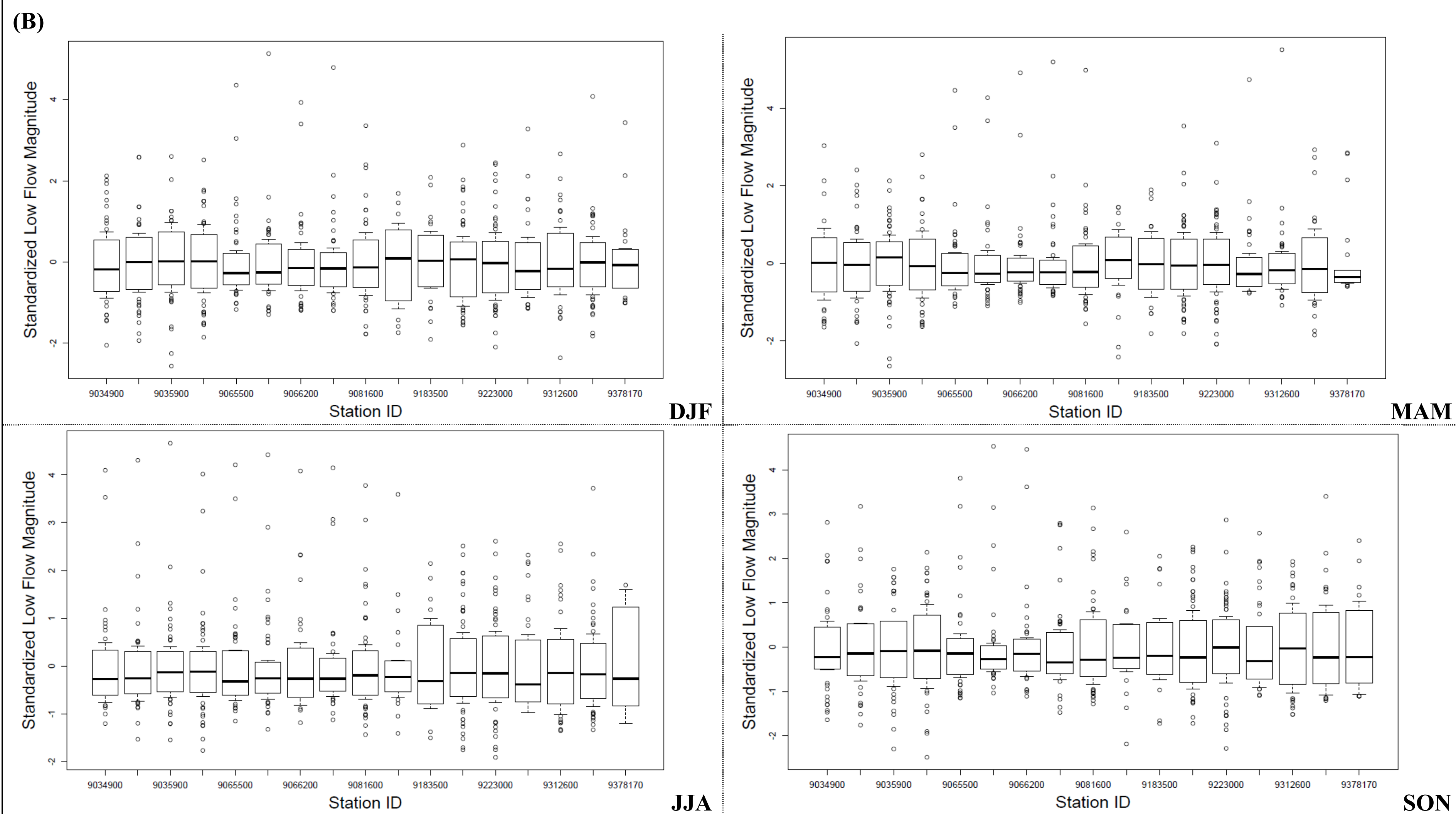

Figure S1: Variability of seasonal q7 (standardized). **(A)** UCRB while all stations pulled together for every year; **(B)** Individual stations, all years pulled together.

(A)

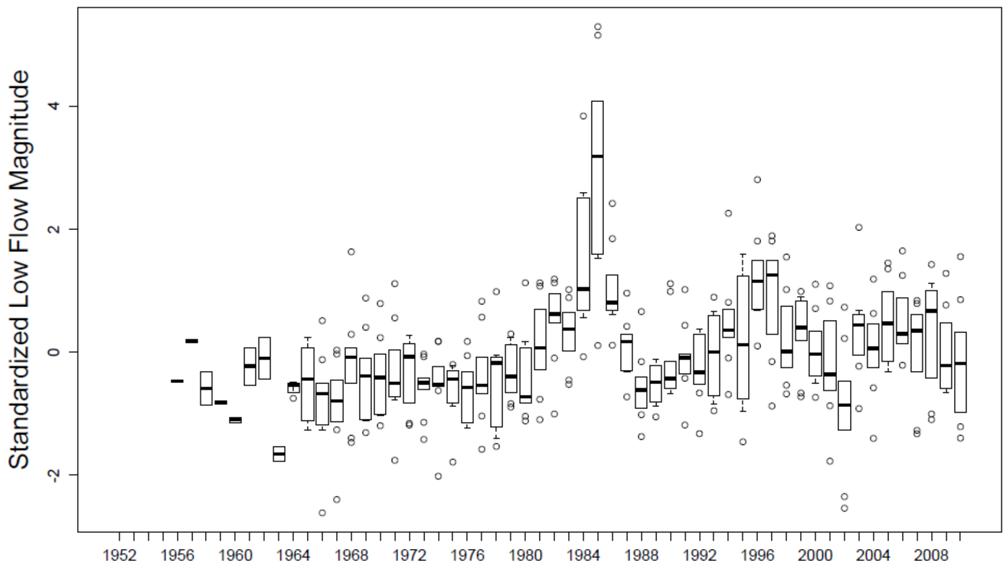

(B)

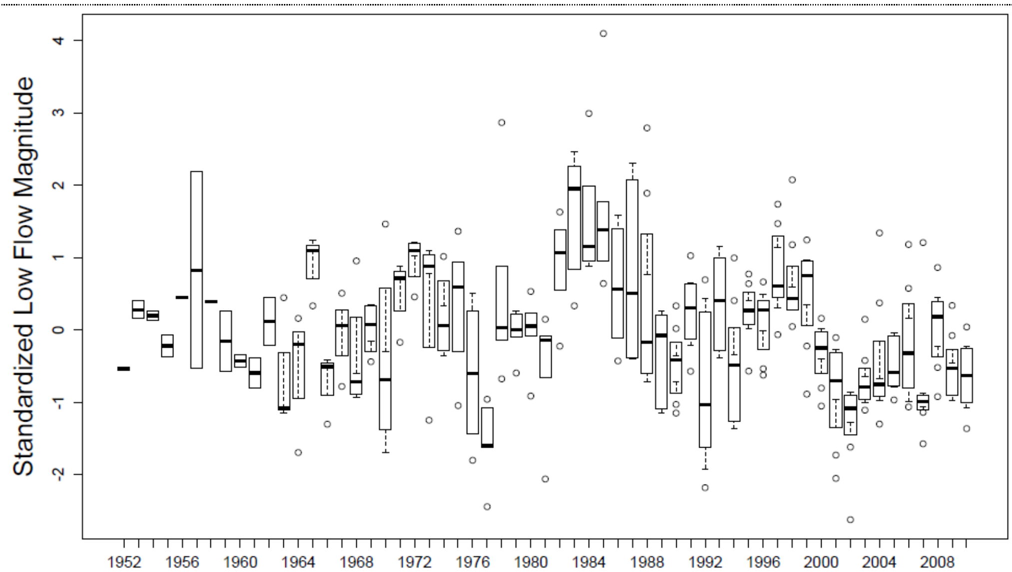

Figure S2: Variability of annual q7 (standardized) of UCRB. **(A)** All "eastern" stations pulled together for every year; **(B)** All "western" stations pulled together for every year.

A)

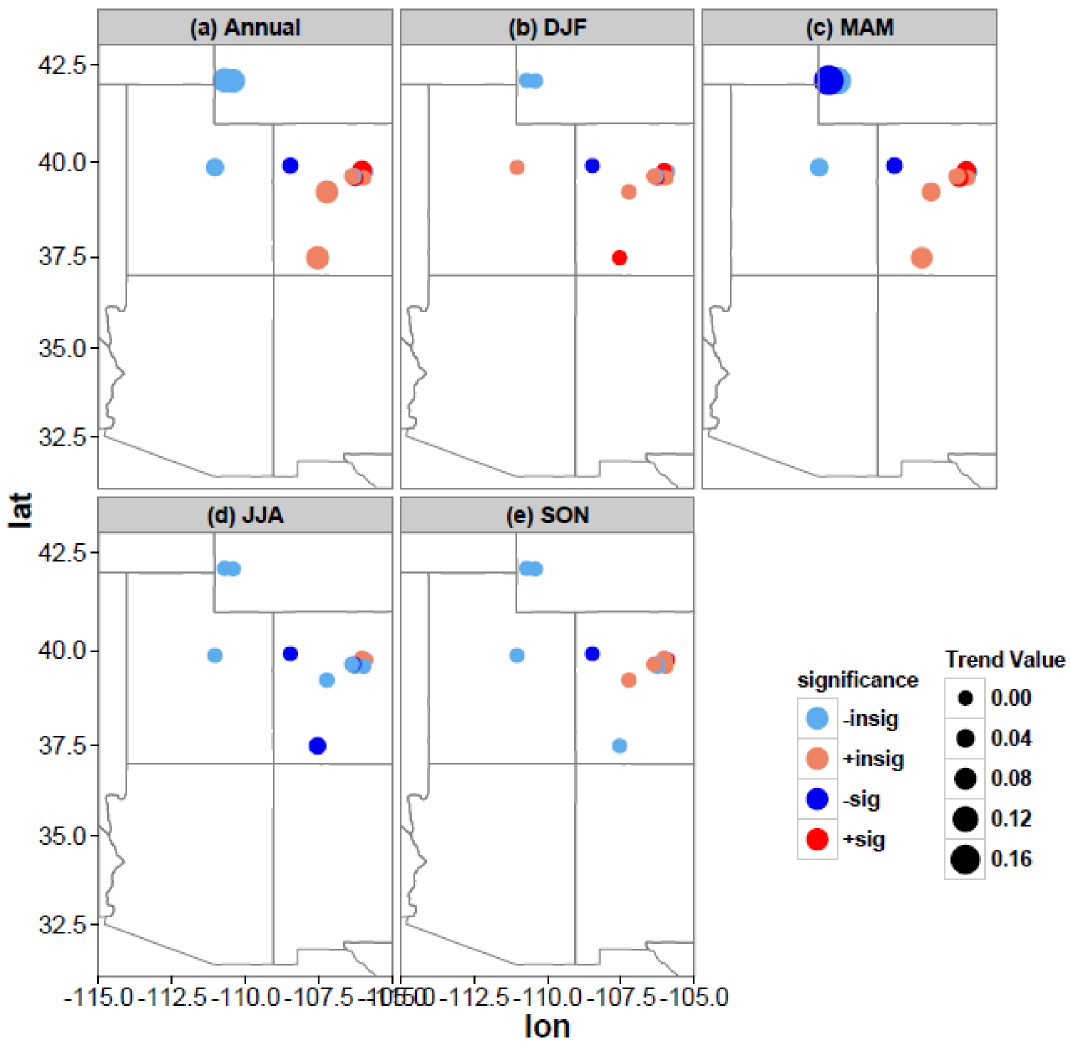

B)

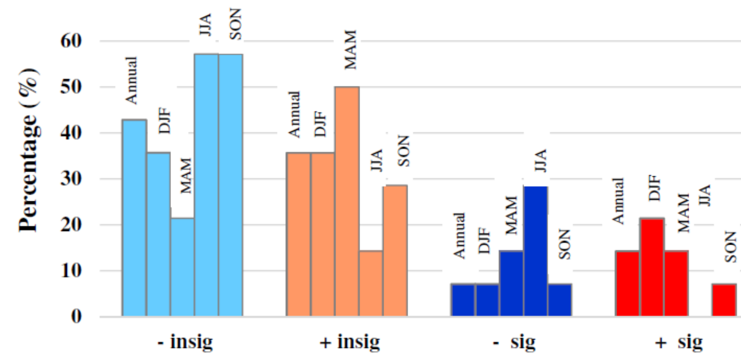

Figure S3: A) Monotonic trends for q7 at each stream-gauge location having more than 30-years data in cms/day/year. (a) Annual, (b) DJF, (c) MAM, (d) JJA, (e) SON. Color bubbles indicate location of each station, sign and significance of the trend estimates. 90% significant levels are used. The size of the bubble is proportional to the magnitude of the trend. **B)** The bar plots of different types of trends in annual and four different seasons.

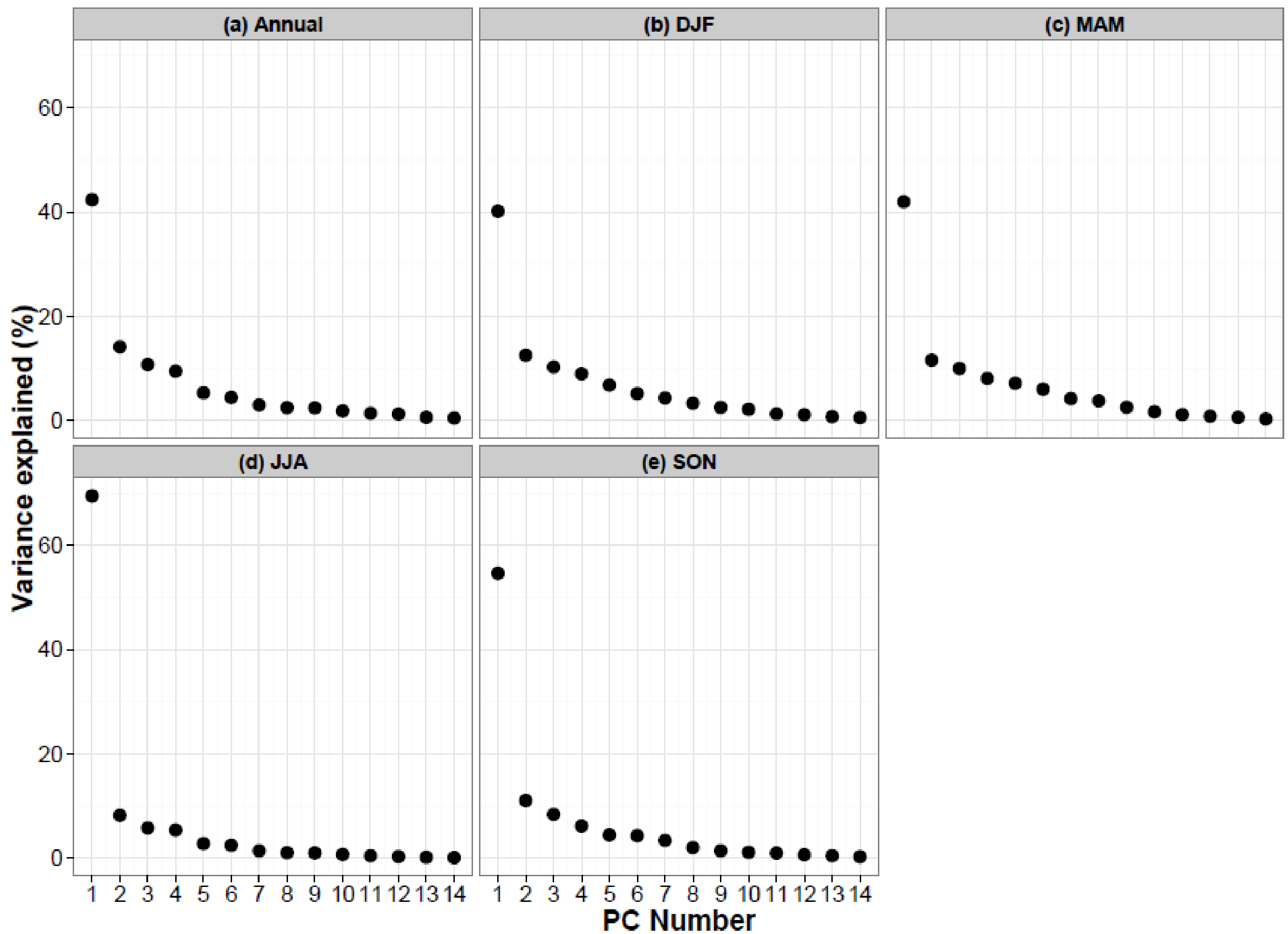

Figure S4: Variance explained by each Principal Component for (a) annual, (b) DJF, (c) MAM, (d) JJA, (e) SON.

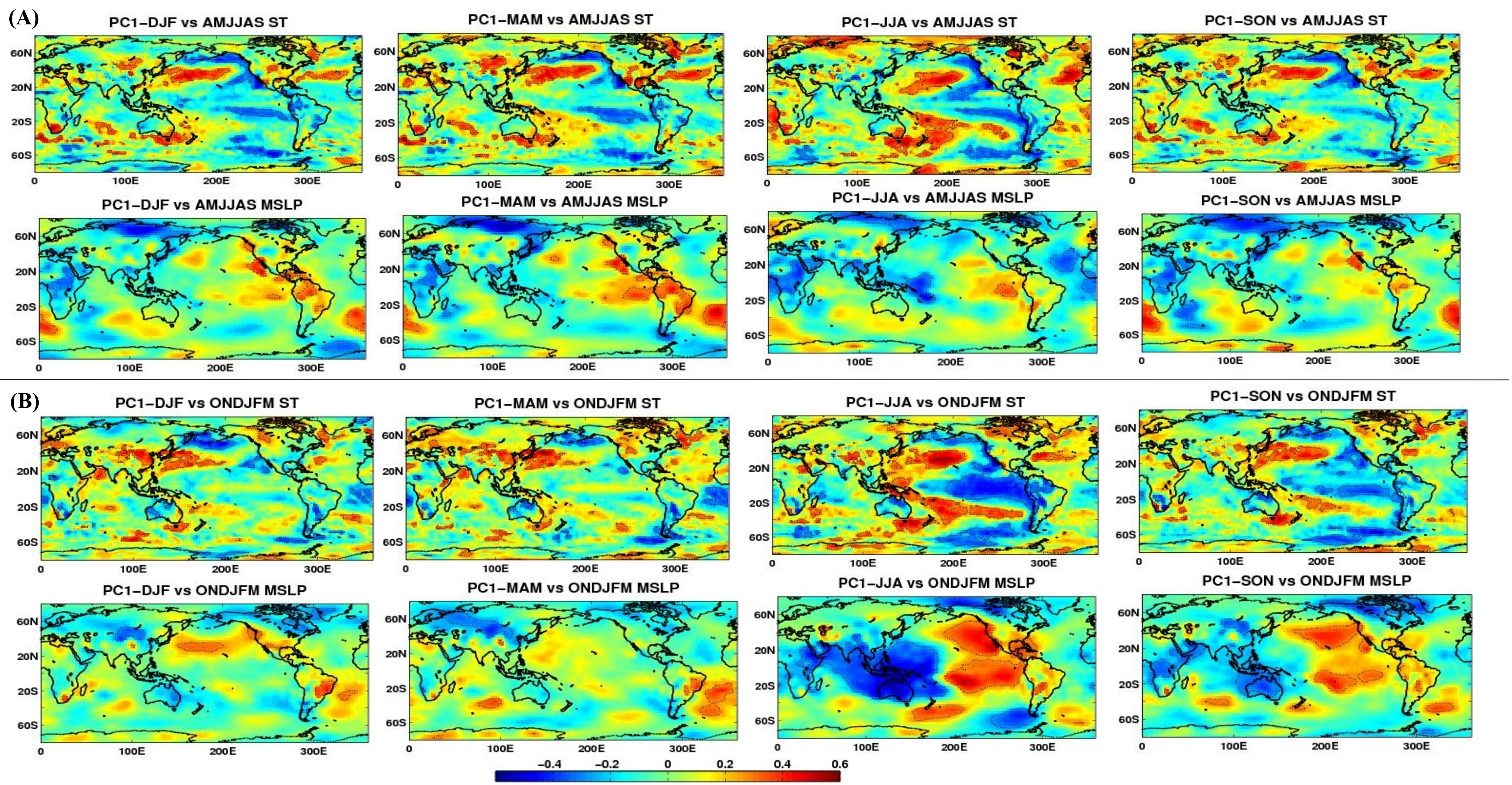

Figure S5: Pearson correlations between PC1 of seasonal q7 with climate data. (**A)** Traditional seasons q7 versus northern summer (AMJJAS) climate, **(B)** Traditional seasons q7 versus northern winter (ONDJFM) **.** (95% significant regions are marked by dotted contours).

Table S1: Occurrence month(s) of annual low flow (q7) for different stream gauge stations in UCRB.

Station ID	Station Name	Annual q7 Occurrence Month(s)
9066000	Black Gore Creek Near Minturn, CO. (east)	Oct-Mar
9034900	Bobtail Creek Near Jones Pass, CO. (east)	Dec-May
9066200	Booth Creek Near Minturn, CO. (east)	Aug-Apr
9306242	Corral Gulch Near Rangely, CO. (west)	Oct-Mar
9081600	Crystal River Ab Avalanche C, Near Redstone, CO. (east)	Nov-Apr
9035800	Darling Creek Near Leal, CO. (east)	Nov-Apr
9065500	Gore Creek At Upper Station, Near Minturn, CO. (east)	Nov-Apr
9047700	Keystone Gulch Near Dillon, CO. (east)	Aug-Apr
9066300	Middle Creek Near Minturn, CO. (east)	Dec-Apr
9035900	South Fork Of Williams Fork Near Leal, CO. (east)	Oct-Mar
9107000	Taylor River At Taylor Park, CO. (east)	Oct-Mar
9352900	Vallecito Creek Near Bayfield, CO. (west)	Oct-Feb
9183500	Mill Creek at Sheley Tunnel, Near Moab, UT. (west)	Jul-Aug & Oct-Feb
9210500	Fontenelle C Nr Herschler Ranch, Nr Fontenelle, WY. (west)	Jul-Aug & Oct-Mar
9223000	Hams Fork Below Pole Creek, Near Frontier, WY. (west)	Jul-Aug & Oct-Feb
9312600	White River Bl Tabbyune C Near Soldier Summit, UT. (west)	Jul-Aug & Oct-Jan
9378170	South Creek Above Reservoir Near Monticello, UT. (west)	Jul-Aug & Oct-Mar
Note: CO = Colorado; UT = Utah; WY = Wyoming; LAT_GAGE = Latitude of a streamgauge; LONG_GAGE = Longitude of a streamgauge.		

Table S2: Summary statistics table for DJF q7 time series for each stream gauge station in UCRB.

Station ID	Station Name	Mean (cms)	Median (cms)	Standard deviation (cms)	Skewness	Kurtosis
9066000	Black Gore Creek Near Minturn, CO. (east)	0.063	0.056	0.029	3.14	15.79
9034900	Bobtail Creek Near Jones Pass, CO. (east)	0.021	0.020	0.004	0.33	-0.46
9066200	Booth Creek Near Minturn, CO. (east)	0.023	0.021	0.012	2.09	6.29
9306242	Corral Gulch Near Rangely, CO. (west)	0.014	0.012	0.011	1.27	1.90
9081600	Crystal River Ab Avalanche C, Near Redstone, CO. (east)	1.222	1.189	0.259	0.95	1.63
9035800	Darling Creek Near Leal, CO. (east)	0.054	0.055	0.012	0.41	0.47
9065500	Gore Creek At Upper Station, Near Minturn, CO. (east)	0.076	0.068	0.033	2.48	7.85
9047700	Keystone Gulch Near Dillon, CO. (east)	0.055	0.055	0.010	0.25	-0.42
9066300	Middle Creek Near Minturn, CO. (east)	0.008	0.007	0.007	2.68	10.75
9035900	South Fork Of Williams Fork Near Leal, CO. (east)	0.210	0.209	0.046	0.14	0.78
9107000	Taylor River At Taylor Park, CO. (east)	0.845	0.858	0.103	-0.30	-0.91
9352900	Vallecito Creek Near Bayfield, CO. (west)	0.490	0.487	0.152	1.21	4.57
9183500	Mill Creek at Sheley Tunnel, Near Moab, UT. (west)	0.138	0.140	0.022	0.17	0.08
9210500	Fontenelle C Nr Herschler Ranch, Nr Fontenelle, WY. (west)	0.553	0.562	0.142	0.46	0.05
9223000	Hams Fork Below Pole Creek, Near Frontier, WY. (west)	0.322	0.320	0.103	0.49	0.14
9312600	White River Bl Tabbyune C Near Soldier Summit, UT. (west)	0.091	0.085	0.035	0.42	0.50
9378170	South Creek Above Reservoir Near Monticello, UT. (west)	0.002	0.002	0.002	2.04	5.32

Note: CO = Colorado; UT = Utah; WY = Wyoming. Highlighted skewness and kurtosis values indicate non-normality of the data.

Table S3: Summary statistics table for MAM q7 time series for each stream gauge station in UCRB.

Station ID	Station Name	Mean (cms)	Median (cms)	Standard deviation (cms)	Skewness	Kurtosis
9066000	Black Gore Creek Near Minturn, CO. (east)	0.076	0.065	0.048	2.91	10.05
9034900	Bobtail Creek Near Jones Pass, CO. (east)	0.020	0.020	0.004	0.48	0.89
9066200	Booth Creek Near Minturn, CO. (east)	0.027	0.024	0.015	3.45	14.36
9306242	Corral Gulch Near Rangely, CO. (west)	0.025	0.016	0.023	1.11	0.01
9081600	Crystal River Ab Avalanche C, Near Redstone, CO. (east)	1.374	1.278	0.377	2.38	10.00
9035800	Darling Creek Near Leal, CO. (east)	0.053	0.052	0.010	0.29	0.01
9065500	Gore Creek At Upper Station, Near Minturn, CO. (east)	0.086	0.075	0.045	2.85	10.07
9047700	Keystone Gulch Near Dillon, CO. (east)	0.054	0.054	0.010	0.47	0.11
9066300	Middle Creek Near Minturn, CO. (east)	0.009	0.007	0.008	3.49	15.65
9035900	South Fork Of Williams Fork Near Leal, CO. (east)	0.207	0.215	0.049	-0.36	0.60
9107000	Taylor River At Taylor Park, CO. (east)	0.906	0.906	0.101	-0.85	1.50
9352900	Vallecito Creek Near Bayfield, CO. (west)	0.605	0.568	0.208	0.92	1.38
9183500	Mill Creek at Sheley Tunnel, Near Moab, UT. (west)	0.145	0.143	0.026	0.30	-0.58
9210500	Fontenelle C Nr Herschler Ranch, Nr Fontenelle, WY. (west)	0.669	0.651	0.170	0.91	1.83
9223000	Hams Fork Below Pole Creek, Near Frontier, WY. (west)	0.402	0.396	0.146	0.26	0.66
9312600	White River Bl Tabbyune C Near Soldier Summit, UT. (west)	0.157	0.139	0.104	4.02	21.19
9378170	South Creek Above Reservoir Near Monticello, UT. (west)	0.010	0.004	0.016	2.27	4.01

Note: CO = Colorado; UT = Utah; WY = Wyoming. Highlighted skewness and kurtosis values indicate non-normality of the data.

Table S4: Summary statistics table for JJA q7 time series for each stream gauge station in UCRB.

Station ID	Station Name	Mean (cms)	Median (cms)	Standard deviation (cms)	Skewness	Kurtosis
9066000	Black Gore Creek Near Minturn, CO. (east)	0.144	0.125	0.072	2.54	8.35
9034900	Bobtail Creek Near Jones Pass, CO. (east)	0.152	0.132	0.079	2.53	8.06
9066200	Booth Creek Near Minturn, CO. (east)	0.076	0.063	0.051	2.08	5.51
9306242	Corral Gulch Near Rangely, CO. (west)	0.025	0.016	0.023	1.11	0.01
9081600	Crystal River Ab Avalanche C, Near Redstone, CO. (east)	3.743	3.418	1.696	1.73	3.83
9035800	Darling Creek Near Leal, CO. (east)	0.141	0.125	0.065	2.31	7.56
9065500	Gore Creek At Upper Station, Near Minturn, CO. (east)	0.341	0.269	0.224	2.54	8.13
9047700	Keystone Gulch Near Dillon, CO. (east)	0.115	0.109	0.049	1.82	5.74
9066300	Middle Creek Near Minturn, CO. (east)	0.046	0.035	0.040	2.77	8.37
9035900	South Fork Of Williams Fork Near Leal, CO. (east)	0.541	0.510	0.207	2.49	10.04
9107000	Taylor River At Taylor Park, CO. (east)	1.867	1.642	0.861	2.22	6.83
9352900	Vallecito Creek Near Bayfield, CO. (west)	2.058	1.881	1.122	1.41	2.90
9183500	Mill Creek at Sheley Tunnel, Near Moab, UT. (west)	0.208	0.184	0.090	0.64	-0.52
9210500	Fontenelle C Nr Herschler Ranch, Nr Fontenelle, WY. (west)	0.842	0.785	0.382	0.65	-0.04
9223000	Hams Fork Below Pole Creek, Near Frontier, WY. (west)	0.549	0.508	0.274	0.41	0.04
9312600	White River Bl Tabbyune C Near Soldier Summit, UT. (west)	0.120	0.106	0.087	0.72	0.09
9378170	South Creek Above Reservoir Near Monticello, UT. (west)	0.003	0.002	0.003	0.50	-1.22

Note: CO = Colorado; UT = Utah; WY = Wyoming. Highlighted skewness and kurtosis values indicate non-normality of the data.

Table S5: Summary statistics table for SON q7 time series for each stream gauge station in UCRB.

Station ID	Station Name	Mean (cms)	Median (cms)	Standard deviation (cms)	Skewness	Kurtosis
9066000	Black Gore Creek Near Minturn, CO. (east)	0.082	0.071	0.040	3.14	10.63
9034900	Bobtail Creek Near Jones Pass, CO. (east)	0.039	0.037	0.009	0.83	0.63
9066200	Booth Creek Near Minturn, CO. (east)	0.036	0.033	0.022	3.04	11.14
9306242	Corral Gulch Near Rangely, CO. (west)	0.018	0.013	0.014	1.00	-0.05
9081600	Crystal River Ab Avalanche C, Near Redstone, CO. (east)	1.776	1.606	0.549	1.27	1.43
9035800	Darling Creek Near Leal, CO. (east)	0.074	0.072	0.020	0.90	1.37
9065500	Gore Creek At Upper Station, Near Minturn, CO. (east)	0.116	0.112	0.043	2.08	5.32
9047700	Keystone Gulch Near Dillon, CO. (east)	0.072	0.071	0.018	-0.07	-0.02
9066300	Middle Creek Near Minturn, CO. (east)	0.016	0.012	0.010	1.57	2.33
9035900	South Fork Of Williams Fork Near Leal, CO. (east)	0.287	0.280	0.065	-0.12	-0.57
9107000	Taylor River At Taylor Park, CO. (east)	1.165	1.096	0.267	0.42	1.47
9352900	Vallecito Creek Near Bayfield, CO. (west)	0.871	0.777	0.400	1.08	1.42
9183500	Mill Creek at Sheley Tunnel, Near Moab, UT. (west)	0.159	0.146	0.049	0.64	-0.01
9210500	Fontenelle C Nr Herschler Ranch, Nr Fontenelle, WY. (west)	0.645	0.599	0.214	0.56	-0.46
9223000	Hams Fork Below Pole Creek, Near Frontier, WY. (west)	0.408	0.409	0.151	0.05	0.35
9312600	White River Bl Tabbyune C Near Soldier Summit, UT. (west)	0.091	0.090	0.058	0.26	-0.95
9378170	South Creek Above Reservoir Near Monticello, UT. (west)	0.002	0.002	0.002	0.77	-0.16

Note: CO = Colorado; UT = Utah; WY = Wyoming. Highlighted skewness and kurtosis values indicate non-normality of the data.

Table S6: Pearson correlation coefficients between DJF q7 time series of different stations. 90% statistically significant estimates are shown.

Station ID	9034900	9066200	9306242	9081600	9035800	9065500	9047700	9066300	9035900	9107000	9352900	9183500	9210500	9223000	9312600	9378170	9034900
9066000																	
9034900																	
9066200																	
9306242																	
9081600	0.38																
9035800					0.42												
9065500		0.41	0.47														
9047700				0.45													
9066300			0.48		0.40												
9035900	0.36				0.41	0.49			0.47								
9107000						0.36											
9352900	0.42			-0.37	0.64												
9183500				0.41	0.41	0.41											
9210500	0.65				0.39			0.39		0.38							
9223000				0.38									0.58	0.39			
9312600			0.36		0.48									0.35			
9378170				0.44				0.36			0.38		0.63		0.36		

Table S7: Pearson correlation coefficients between MAM q7 time series of different stations. 90% statistically significant estimates are shown.

Station ID	9034900	9066200	9306242	9081600	9035800	9065500	9047700	9066300	9035900	9107000	9352900	9183500	9210500	9223000	9312600	9378170	9034900
9066000																	
9034900																	
9066200																	
9306242																	
9081600																	
9035800																	
9065500			0.43														
9047700				0.35													
9066300			0.46														
9035900									0.43								
9107000																	
9352900		-0.52			0.57												
9183500				0.52								0.51					
9210500																	
9223000													0.60	0.41			
9312600												0.41	0.37				
9378170		-0.48			0.52	-0.35				-0.43		0.65				0.40	

Table S8: Pearson correlation coefficients between SON q7 time series of different stations. 90% statistically significant estimates are shown.

Station ID	9034900	9066200	9306242	9081600	9035800	9065500	9047700	9066300	9035900	9107000	9352900	9183500	9210500	9223000	9312600	9378170	9034900
9066000																	
9034900																	
9066200																	
9306242																	
9081600	0.64																
9035800	0.49			0.39	0.74												
9065500	0.42		0.51		0.66	0.49											
9047700	0.65				0.50	0.44											
9066300			0.48		0.52	0.53	0.56	0.47									
9035900	0.80				0.70	0.53	0.57	0.59	0.62								
9107000	0.53		0.54	0.36	0.65	0.59	0.81	0.50	0.51	0.62							
9352900																	
9183500	0.49			0.68	0.57	0.68		0.37			0.53						
9210500	0.62			0.47	0.57	0.44		0.37		0.58	0.48		0.50				
9223000	0.70			0.37	0.55	0.48		0.42		0.63	0.39		0.43	0.86			
9312600	0.66			0.63	0.71	0.77	0.53	0.47	0.41	0.62	0.74		0.78	0.74	0.69		
9378170	0.45	-0.37		0.56	0.35	0.56					0.40		0.77	0.49	0.49	0.63	

Table S9: Periodicities identified (in number of years) for annual q7 magnitude for different stream gauge locations.

Station ID	Station Name	Active years identified	Periodicity in years (within the cone of influence)
9066000	Black Gore Creek Near Minturn, CO. (east)		
9034900	Bobtail Creek Near Jones Pass, CO. (east)		
9066200	Booth Creek Near Minturn, CO. (east)		
9306242	Corral Gulch Near Rangely, CO. (west)		
9081600	Crystal River Ab Avalanche C, Near Redstone, CO. (east)	1967-2003	12 - 16
9035800	Darling Creek Near Leal, CO. (east)	1978-1990 1980- 2000	6 - 8 15
9065500	Gore Creek At Upper Station, Near Minturn, CO. (east)	1976-2000	10 - 15
9047700	Keystone Gulch Near Dillon, CO. (east)		
9066300	Middle Creek Near Minturn, CO. (east)		
9035900	South Fork Of Williams Fork Near Leal, CO. (east)		
9107000	Taylor River At Taylor Park, CO. (east)		
9352900	Vallecito Creek Near Bayfield, CO. (west)		
9183500	Mill Creek at Sheley Tunnel, Near Moab, UT. (west)	1996-2004	5 - 7
9210500	Fontenelle C Nr Herschler Ranch, Nr Fontenelle, WY. (west)	1974-2003	13- 16
9223000	Hams Fork Below Pole Creek, Near Frontier, WY. (west)	1971- 2003	10 - 16
9312600	White River Bl Tabbyune C Near Soldier Summit, UT. (west)	1975-1995	12-16
9378170	South Creek Above Reservoir Near Monticello, UT. (west)		

Table S10: Periodicities identified (in number of years) for seasonal q7 magnitudes for different stream gauge locations.

Station ID	Station Name	DJF		MAM		JJA		SON	
		Active years identified	Period	Active years identified	Period	Active years identified	Period	Active years identified	Period
9066000	Black Gore Creek Near Minturn, CO. (east)								
9034900	Bobtail Creek Near Jones Pass, CO. (east)					1983-1984 1975-1990	4-5 6-16		
9066200	Booth Creek Near Minturn, CO. (east)								
9306242	Corral Gulch Near Rangely, CO. (west)			-		1989-1998	12-14		
9081600	Crystal River Ab Avalanche C, Near Redstone, CO. (east)	1968-2003	12 - 16			1994 - 1996 1980-2005	2 -3 10-15	1973-2001	10 - 16
9035800	Darling Creek Near Leal, CO. (east)	1975-1988 1979-1999	6-9 12-16	1977-1997 2005-2008	6-8 2.5-3	1983-1987 1975-1990	3.5-5 9-15	1976-1995	12-15
9065500	Gore Creek At Upper Station, Near Minturn, CO. (east)			1982-1986	3-4			1971-1993	10-16
9047700	Keystone Gulch Near Dillon, CO. (east)								
9066300	Middle Creek Near Minturn, CO. (east)							1977-1991	13-15
9035900	South Fork Of Williams Fork Near Leal, CO. (east)	1989-2011	11-15			1975-2000	10-15	1978-2011	11-14
9107000	Taylor River At Taylor Park, CO. (east)			1998-2005	2-4				
9352900	Vallecito Creek Near Bayfield, CO. (west)	1979-2005	10-12						
9183500	Mill Creek at Sheley Tunnel, Near Moab, UT. (west)								
9210500	Fontenelle C Nr Herschler Ranch, Nr Fontenelle, WY. (west)	1988-2003	13- 15			1981-1986 1981-2010	3-4 12-16	1977-2003	12-16
9223000	Hams Fork Below Pole Creek, Near Frontier, WY. (west)	1967-1972 1973-1982	3-4 8-10						
9312600	White River Bl Tabbyune C Near Soldier Summit, UT. (west)	1974-1993	10-15	1984-1987 1980-1993	2.5-3.5 8-15	1977-1996	11-15	1977-1998	11-15
9378170	South Creek Above Reservoir Near Monticello, UT. (west)								